Carbohydrate Polymers 86 (2011) 1157–1166

Contents lists available at ScienceDirect

Carbohydrate Polymers

journal homepage: www.elsevier.com/locate/carbpol

Low molecular weight heparin-all-*trans*-retinoid acid conjugate as a drug carrier for combination cancer chemotherapy of paclitaxel and all-*trans*-retinoid acid

Lin Hou [a], Ying Fan [a], Jing Yao [a,*], Jianping Zhou [a,**], Caocao Li [a], Zhengjie Fang [a], Qiang Zhang [b]

[a] *Department of Pharmaceutics, China Pharmaceutical University, 24 Tongjiaxiang, Nanjing 210009, China*
[b] *Pharmaceutical Sciences Department, Peking University, 38 Xueyuan Road, Haidian District, Beijing 100191, China*

ARTICLE INFO

Article history:
Received 19 February 2011
Received in revised form 28 May 2011
Accepted 6 June 2011
Available online 15 June 2011

Keywords:
Low molecular weight heparin
Paclitaxel
All-*trans*-retinoid acid
Conjugates
Self-assembled nanoparticles
Combination therapy

ABSTRACT

As a novel nanocarrier for simultaneous delivery of multiple anticancer drugs, low molecular weight heparin-all-*trans*-retinoid acid (ATRA) (LHR) conjugate was developed. Amphiphilic LHR conjugate had markedly lower anticoagulant activity, and could self-assemble to form nanoparticles for loading hydrophobic drugs. The critical aggregation concentrations of LHR conjugates were varied from 407 to 40 mg/L. Paclitaxel (PTX)-loaded LHR nanoparticles were prepared by the dialysis method, with particle sizes in the range of 228.0–108.9 nm. The maximum drug-loading was as much as 33.1% with an entrapment efficiency of 93.1%. They displayed enhanced PTX-induced cytotoxicity to HepG2 cells compared to PTX solution. Hemolysis and cytotoxicity studies showed that LHR conjugate was a safe material for intravenous administration. Moreover, the pharmacokinetic profiles indicated that PTX-loaded LHR nanoparticles contributed to an extended circulation of PTX and ATRA. These results suggest that PTX-loaded LHR nanoparticles can be considered as promising anticancer drug delivery system for combination chemotherapy.

1. Introduction

Paclitaxel (PTX) is known as one of the most exciting anti-cancer drugs in the market today. Significant antitumor activity has been demonstrated in clinical trials against a wide variety of tumors, including ovarian carcinoma, breast cancer, head and neck cancers and non-small cell lung cancer (Rowinsky & Donehover, 1995). So far, several drug delivery systems (DDS) for PTX have successfully improved its therapeutic profile, such as liposomes (Ceruti et al., 2000), nanoparticles (Hawkins, Soon-Shiong, & Desai, 2008), parenteral emulsion (Kan, Chen, Lee, & Chu, 1999) water-soluble prodrugs and conjugates (Safavy et al., 2003). However, due to the heterogeneity of cancer cells as well as acquired drug resistance, single agent therapy is limited and combination chemotherapy has become a standard regimen to treat cancer patients. Unlike single-agent therapy, combination therapy can modulate different signaling pathways in cancer cells, maximize the therapeutic effect and, possibly, overcome mechanisms of resistance (Muindi, 1996). Accordingly, the promising clinical activity of PTX has promoted considerable interest in combining it with other anti-tumor agents, such as topotecan (Tiersten et al., 2004) and S-1 (Ueda et al., 2010).

Recently, an increasing amount of attention has been paid to the combination of PTX with all-*trans*-retinoid acid (ATRA). ATRA, one of the retinoids, inhibits cell proliferation and induces differentiation in a variety of tumor cell lines *in vitro* (Sun et al., 2005). It has previously been reported that ATRA could enhance PTX-induced cytotoxicity by reducing surviving expression in MCF-7 cells and preventing PTX-mediated induction of surviving expression (Pratt, Niu, & Renart, 2006). Karmakar, Banik, and Ray (2008) also found that combination of ATRA with PTX caused regression of tumor by down regulation of survival factors and activation of mitochondria-dependent multiple molecular mechanisms for apoptosis. Besides, a recent study suggested that the combination of ATRA with the standard chemotherapy regimen was a safe and potentially useful treatment for non-small-cell lung carcinoma (Arrieta et al., 2010). Therefore, the combination of PTX with ATRA may be a feasible strategy to enhance the effects of chemotherapy.

However, PTX and ATRA are water-insoluble, and mixed drugs are prone to aggregation and precipitation, losing respective pharmaceutical activity and raising a risk of embolisms (Bae, Diezi, Zhao, & Kwon, 2007). Currently, these obstacles cannot be overcome by conventional drug formulations, necessitating sequential drug administration or a separate IV line. Polymer-drug conjugate is considered as a promising DDS to overcome these limitations (Greco & Vicent, 2009) as well as for increasing water-solubility and chemical stability, improving pharmacokinetic and distribution profile, reducing side effects and, sometimes, targeting disease

* Corresponding author. Tel.: +86 25 83271102; fax: +86 25 83301606.
** Corresponding author. Tel.: +86 25 83271102.
E-mail addresses: yaoj3@163.com (J. Yao), zhoujpcpu@126.com (J. Zhou).

0144-8617/$ – see front matter © 2011 Elsevier Ltd. All rights reserved.
doi:10.1016/j.carbpol.2011.06.008

site either by active or passive mechanisms (Garnett, 2001). Miller et al. (Segal & Satchi-Fainaro, 2009) conjugated two drugs with the same polymeric backbone resulting in a nano-conjugate at a size of ~100 nm. A phase I study was carried out on 43 patients with advanced solid tumors combining a fixed dose of *cis*-platin with escalating doses of PGA–PTX. Hence, PTX and ATRA might be incorporated into a single polymer–drug conjugate nanoparticles system for the multiple drugs delivery simultaneously.

Polymer for preparing the conjugates should ideally be water-soluble, non-toxic, and non-immunogenic, as well as degraded and/or eliminated from the organism (Godwin et al., 2001; Rihova, 2002). Heparin has attracted intense attention because it is not only a biocompatible, biodegradable, and water-soluble natural polysaccharide with a complicated structure and is abundant in animal tissues, but also it demonstrates a variety of biological activities including anticoagulant activity, inhibition of tumor growth and angiogenesis (Wang, Xin, Liu, Zhu, & Xiang, 2009). Herein, low molecular weight heparin (LMWH) with superior safety, pharmacokinetics, efficacy and convenience is an excellent choice for such trials (Zacharski & Ornstein, 1998). It was reported that LMWH and its derivatives, chemically modified with hydrophobic segments could reduce the risk of hemorrhage and prevent metastasis, angiogenesis and tumor growth or cancer cell proliferations (Park, Kim, et al., 2008). These LMWH derivatives have been suggested to be safe drug carriers and also as effective drugs for cancer therapy (Go, Joung, Park, Park, & Park, 2008; Jee, Park, Park, Kim, & Shin, 2004; Lee, Nam, Shin, & Byun, 2001). Park, Lee, et al. (2008) has described that the hepain–deoxycholic acid (HD) conjugate had a potent antiangiogenic effect and the safety for long-term treatment. Besides, doxorubicin-loaded HD nanoparticles displayed enhanced cytotoxic effects and apoptosis.

In this study, we synthesized a LMWH-ATRA (LHR) conjugate, by covalently bonding aminated ATRA to LMWH via amide formation, for potentially synergistic combination cancer chemotherapy. Because of reserving the active groups including the extended polyene chain and cyclohexenyl of ATRA (Sadikoglou et al., 2009) as well as the intact sulfate group of LMWH (Park et al., 2006), this amphiphilic conjugate was expected to possess anticancer activity and could self-assemble into nanoparticles for loading PTX. Characterization and stability of the PTX-loaded LHR nanoparticles were evaluated. In addition, by analyzing drug release profile, hemolysis and cytotoxicity *in vitro*, and by addressing the pharmacokinetics, we here provide a novel DDS with sustained release characteristics, improved safety, enhanced antitumor activity and optimized pharmacokinetic profile.

2. Materials and methods

2.1. Materials

Low molecular weight heparin (LMWH, 100 IU/mg), average molecular weight near 4500 Da, was obtained from Nanjing University. Paclitaxel (PTX) and all-*trans*-retinoid acid (ATRA) were purchased from Chongqing Melian Pharmaceuticals Co., Ltd. (Chongqing, China) and Wuhan Hezhong Bio-Chemical Manufacture Co., Ltd. (Hunan, China), respectively. Anhydrous dimethylformamide (DMF), anhydrous formamide and 1-ethyl-3-(3-dimethylaminopropyl)-carbodiimide (EDC) were from Shanghai Lingfeng Chemical Reagent Co., Ltd. (Shanghai, China) and Sigma Chemical Co. (St. Louis, MO), respectively. *N*-Hydroxysuccinimide (NHS), *N*,*N*-dicyclohexyl carbodiimide (DCC) and pyrene were from Sinopharm Chemical Reagent Co. Ltd. (Nanjing, China). All other chemicals were of analytical grade and were used without further purification.

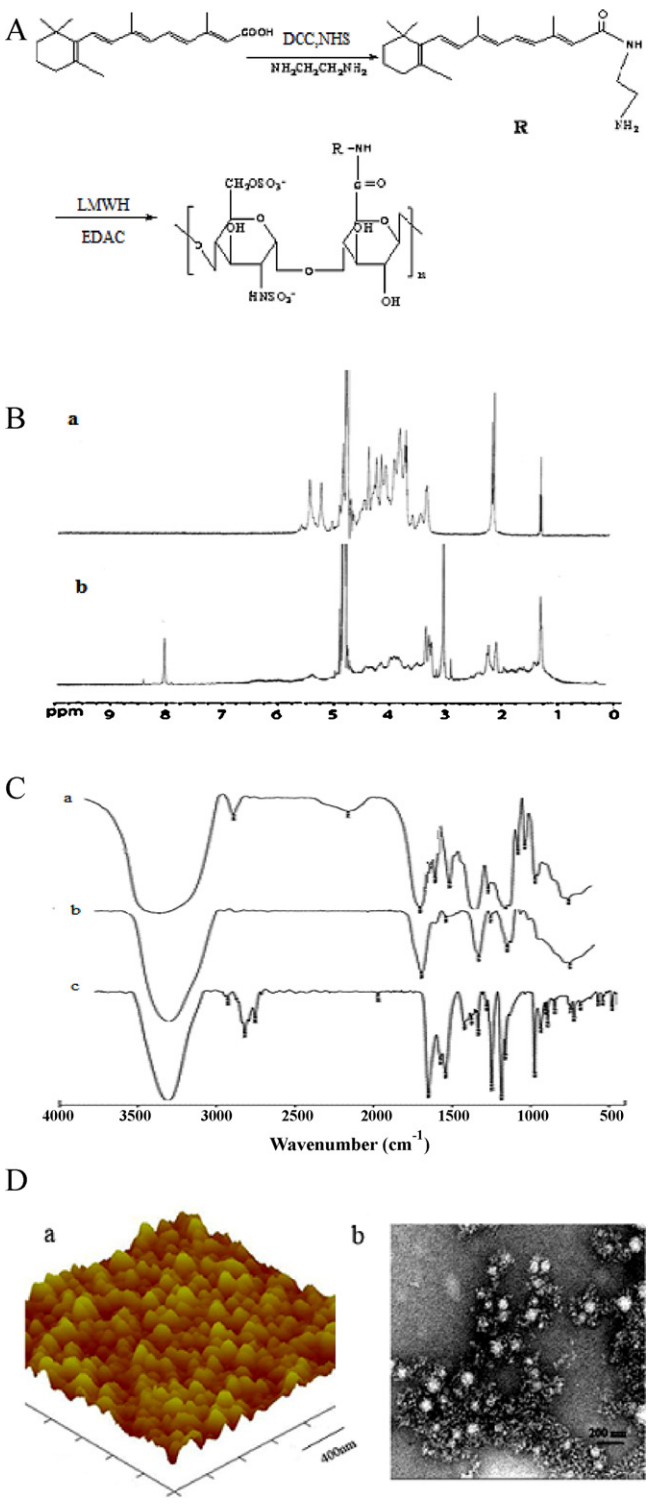

Fig. 1. Preparation and characterization of the LHR conjugate: (A) synthetic scheme for LHR conjugates; (B) ^{1}H NMR spectra of (a) LMWH and (b) LHR conjugate in D_2O, respectively; (C) FTIR spectra of (a) LHR, (b) LMWH and (c) ATRA, respectively; (D) (a) AFM and (b) TEM images of LHR nanoparticles.

2.2. Synthesis of the LHR conjugate

The LHR conjugate was synthesized by coupling LMWH with aminated ATRA (Fig. 1(A)). Firstly, ATRA (7 mmol) in 20 mL DMF was reacted with DCC (10.5 mmol) and NHS (8.4 mmol) for overnight at ambient temperature. After reaction, the precipitant was filtrated off and washed several times with acetic ether. Then,

the filtrate was washed, followed by evaporation of the solvent. The succinimido ATRA was obtained. To an ice-cold solution of ethylenediamine (9 mmol) in dichloromethane (DCM) (20 mL), solution of the succinimido ATRA (3 mmol) was added dropwise over 1 h. The reaction mixture was washed sequentially with an ice-cold 5% aqueous, $NaHCO_3$ and brine. Finally, pure ATRA-NH_2 was obtained by silica gel column chromatography.

Secondly, LMWH (0.1 g) was dissolved in formamide (5 mL) by gentle heating. Different amounts of EDC were mixed with LMWH solutions at room temperature, followed by the addition of different amounts of ATRA-NH_2 dissolved in DMF (5 mL). After 24 h, the mixture was precipitated in excess cold acetone, and the precipitate was carefully washed three times with acetone to remove excess ATRA-NH_2. The dried LHR conjugate was dissolved in water and then dialyze against deionized water for 48 h using a dialysis membrane (MWCO 1000), followed by lyophilization.

2.3. Characterization of the LHR conjugate

The chemical structure of LHR conjugate was characterized by ^{1}H NMR and FTIR spectra. The degree of substitution (DS), defined as the number of ATRAs per LMWH molecule, was estimated by UV measurements based on a standard curve generated with known concentrations of ATRA in ethanol (λ = 345 nm).

The critical aggregation concentration (CAC) of LHR conjugate was estimated by the fluorescence spectroscopy, using pyrene as the probe. Briefly, 1 mL of 6.0×10^{-6} M pyrene solution in acetone was added to a series of 10 mL volumetric flasks and then acetone was evaporated. 10 mL of different concentrations of LHR conjugate solutions (1×10^{-4} to 5 mg/mL) was added to the volumetric flasks followed by sonicating for 30 min. The samples were incubated at 65 °C for 1 h, and then left to cool down overnight at room temperature. Fluorescence spectra were recorded with a RF-5301 PC florescence spectrophotometer (Shimadzu, Japan) with the emission wavelength at 390 nm. Both of the excitation and emission slit-widths were 3 nm. The CAC was estimated as the cross-point when extrapolating the intensity ratio I_{338}/I_{333} at low and high concentration regions.

Anticoagulant activity of LHR conjugates was determined by the established procedures of the bioactivity assays such as FXa chromogenic and aPTT assays, respectively (Lee, Moon, & Byun, 1998).

2.4. Preparation and characterization of PTX-loaded LHR nanoparticles

To prepare the LHR nanoparticles, amphiphilic LHR conjugates were dissolved in water and the solution was sonicated for 10 min using a probe-type ultrasonicator (JY 92-2D; Ningbo Scientz Biotechnology Co., Ltd, Nanjing, China) at 100 W. The resulting solution was centrifuged at 3000 rpm for 10 min followed by filtration through a 0.45 μm membrane filter. The LHR nanoparticles were characterized with respect to their size and zeta potential by dynamic light scattering (DLS) using a Malvern Zetasizer Nano-ZS90. The morphology of LHR nanoparticles was observed by atomic force microscopy (AFM, Nano Scope IIIa, Veeco, USA) and transmission electron microscopy (TEM, H-600, Hitachi, Japan).

PTX-loaded LHR nanoparticles were prepared by a dialysis method. 18 mg of LHR conjugate was dissolved in 3 mL of water with stirring for 30 min at room temperature. Then the solution was added with 10 mg of PTX at the concentration of 30 mg/mL in ethanol followed by 15 min of stirring, and the solution was ultrasonicated for 30 min in ice-bath by a probe-type ultrasonicator (JY92-2D, Ningbo Scentz Biotechnology Co., Ltd., China). The solution was dialyzed against an excess amount of distilled water with a dialysis bag (MWCO 1000) overnight followed by centrifugation at 3000 rpm for 10 min, filtering through a 0.45 μm pore-sized microporous membrane and lyophilizing. The particle size, size distribution and zeta potential of PTX-loaded LHR nanoparticles were determined by DLS. Differential scanning calorimeter (DSC) analysis was carried out using NETZSCH DSC 204 equipment with the temperature range and heating rate of 40–300 °C and 10 °C/min, respectively.

The amount of PTX in the nanoparticles was measured by high performance liquid chromatography (HPLC, Shimadzu LC-2010 system, Kyoto, Japan) with UV detection at 227 nm. The drug-loading (DL) and entrapment efficiency (EE) of PTX were calculated by the following equations:

$$\mathrm{DL}(\%) \frac{\text{weight of PTX in nanoparticles}}{\text{weight of PTX in nanoparticles} + \text{weight of LHR fed initially}} \times 100$$

$$\mathrm{EE}(\%) = \frac{\text{weight of PTX in nanoparticles}}{\text{weight of PTX fed initially}} \times 100$$

2.5. In vitro drug(s) release studies

The release profiles of PTX and ATRA from PTX-loaded LHR nanoparticles and PTX plus ATRA solution were evaluated by a dialysis method. The lyophilized PTX-loaded LHR nanoparticles were dispersed in 5% glucose solution, to yield about 0.50 mg/mL of PTX and 0.10 mg/mL ATRA (according to the amount of PTX and ATRA in PTX-loaded LHR nanoparticles). PTX plus ATRA solution was prepared by dissolving 12 mg of PTX and 2.4 mg of ATRA in ethanol with an equal volume of cremophor EL, followed by dilution to obtain the equivalent PTX and ATRA concentration of 0.50 mg/mL and 0.10 mg/mL. A volume of 1 mL the prepared sample was placed in a dialysis tube (MWCO 12000) and was tightly sealed. Then, the tube was immersed in 150 mL of PBS at pH 7.4, and gently shaken at 37 °C in a water bath at 100 rpm. The release samples (5 mL) were obtained at different time intervals and the medium was refreshed. In addition, the release of the nanocarrier in acidic media (pH ~5.8) was also initially investigated as above.

The drugs were determined by a reported method (Zeng et al., 2005). PTX and ATRA in the release samples were extracted by using 2 mL of DCM, dried under a stream of nitrogen, and reconstituted in 100 μL of methanol. The concentration of PTX and ATRA were determined by HPLC analysis.

2.6. Hydrolysis study of LHR nanoparticles and stability of PTX-loaded LHR nanoparticles in plasma

The hydrolysis study of LHR nanoparticles was carried out by the addition of 10 mg LHR conjugate in 1 mL of plasma and the samples were incubated at 37 °C with mild stirring. At predetermined times, 150 μL of sample was taken and centrifuged to obtain the 100 μL of supernatant solution. Then, ATRA was extracted with 2 mL of methyl *tert*-butyl ether and analyzed using the LC/MS system. Liquid chromatography (LC) was performed using a Shimadzu LC-10AD HPLC system equipped with an autosampler (SIL-HTc) and was coupled to a Shimadzu LCMS-2010A quadrupole mass spectrometer with an electrospray ionization (ESI) interface. The ESI in positive ion mode was adopted for the analytes quantitation with the following parameters: $[M+H]^+$ m/z at 301.15 for ATRA.

For the stability study of the PTX-loaded LHR nanoparticles in plasma, 3 mL of nanoparticle solution (0.5 mg/mL of PTX) was added to 3 mL of 50% rat plasma following the process similar to that of ATRA. PTX was extracted from plasma by adding 10 mL of methanol. After centrifugation, the supernatant was analyzed by previously described HPLC method.

2.7. In vitro cytotoxicity studies

The cytotoxicity of PTX-loaded LHR nanoparticles was assessed using the MTT assay. The HepG2 (hepatocellular carcinoma, human) cells were seeded at a density of 1×10^5 cells/well in 96-well microtitre plates and incubated for 24 h. The cells were then treated with the PTX-loaded LHR nanoparticles, LHR conjugate, PTX solution and PTX plus ATRA solution (all performed at equivalent PTX and ATRA concentration of 0.01, 0.1, 1, 10 and 100 μg/mL, and 0.002, 0.02, 0.2, 2 and 20 μg/mL, respectively) for 72 h, respectively. PTX solution, which is a commercial formulation, was prepared by dissolving 200 μL of 12 mg/mL PTX in ethanol with an equal volume of cremophor EL, followed by sonication for 30 min (Sato, Wang, Adachi, & Horikoshi, 1996). PTX plus ATRA solution was prepared as the same procedure but with the addition of ATRA (2.4 mg/mL) in ethanol. After incubation, MTT solution (20 μL, 5 mg/mL in PBS) was then added to each well and the cells were incubated further for 4 h at 37 °C. The media were removed and the cells were dissolved in DMSO. Absorbance at 570 nm was measured with a microplate reader (SOFT max™ PRO, Molecular Devices Corporation, CA). Cell viability (%) was calculated as (OD of test group/OD of control group) × 100.

2.8. Hemolysis test

The hemolysis test was performed as described previously (Le Garrec et al., 2004). The concentration of rabbit red blood cells (RBC) was fixed to 2% (v/v). The LHR conjugate and PTX-loaded LHR nanoparticles were dissolved in 5% glucose injection solution at a concentration of 10 mg LHR/mL, 0.5 mg PTX/mL and 0.1 mg ATRA/mL. 2.5 mL of 2% RBC suspension was added to each tube which contained different volumes (0.1–2 mL) of LHR conjugate or PTX-loaded LHR nanoparticles solution. Then 5% glucose injection solution was added in each tube to obtain a final volume of 5 mL.

The positive (100% hemolysis) and negative control (0% hemolysis) were obtained by mixing 2.5 mL of water and 5% glucose injection solution with 2.5 mL of 2% RBC suspension to eliminate the effect of background. For comparison, the mixture of cremophor EL and ethanol (v/v, 1:1), the commonly used low-molecular weight surfactant Tween-80 solution and the PTX plus ATRA solution were also prepared, respectively. Samples were incubated at 37 °C for 1 h, and centrifuged at 3000 rpm for 10 min to remove non-lysed RBC. The supernatant was analyzed by spectrophotometric determination at 540 nm. The degree of hemolysis was determined by the following equation:

$$\text{Hemolysis} = \frac{A_{\text{sample}} - A_{0\%}}{A_{100\%} - A_{0\%}} \times 100$$

2.9. Pharmacokinetic study

PTX-loaded LHR nanoparticles or PTX plus ATRA solution were intravenously administered via a tail vein to Sprague–Dawley rats at a dose of 8 mg PTX/kg and 1.6 mg ATRA/kg. At predetermined times (5 min, 10 min, 15 min, 30 min, 1, 2, 4, 8, 12, 24, 36 and 48 h) after the intravenous (i.v.) injection, blood samples (0.5 mL) were taken immediately from retro-orbital plexus, and then centrifuged to separate the plasma and stored at −20 °C until analysis.

The extraction of PTX and ATRA from plasma was carried out as follows: 15 μL of docetaxel (internal standard) (100 μg/mL in methanol) was added to 10 mL centrifuge tubes and evaporated until dry; 150 μL of plasma sample was added and vortex mixed, and extracted with 4 mL of methyl *tert*-butyl ether for 5 min. After centrifugation, 3 mL of the organic layer was transferred to a glass tube and evaporated to dryness. The residue was dissolved in 100 μL of methanol by vortexing and 10 μL was analyzed using LC/MS system.

PTX and ATRA concentrations were measured by LC/MS (Shimadzu LCMS-2010A system, Kyoto, Japan). Separation of analytes was carried out on a Shim-pack C_{18} column (150 mm × 2.0 mm, 5 μm, Shimadzu). The mobile phases were constituted with solvent A: water containing 0.1% formic acid, and solvent B: 100% methanol. The flow rate was set to 0.2 mL/min, and column temperature to 35 °C. Linear gradient elution was employed with a 15 min run time.

The pharmacokinetic parameters were calculated from the average PTX and ATRA concentrations in the bloodstream using Kinetic 4.4.1.

2.10. Statistics

All the data were presented as mean ± SD from three to eight independent measurements in separate independent experiments and analyzed using descriptive statistic and single-factor analysis of variance.

3. Results

3.1. Preparation and characterization of the LHR conjugate

The composition of synthesized conjugate was analyzed by ^{1}H NMR and FTIR. The new amide linkages between LMWH and ATRA and the intrinsic sulfonamide in LMWH appeared at 8.04 and 5.3 ppm, respectively. The characteristic peaks of ATRA appeared at 1.0–1.6 ppm (Fig. 1(B)). In the FTIR spectra (Fig. 1(C)), the peaks at 1627 cm^{-1} further confirmed the new amide linkages. In addition, compared to free LMWH, the peak of the stretching vibration of intrinsic sulfonamide (–$NHSO_3$) in LMWH of the conjugate was observed at near 2136 cm^{-1} as reported by some researchers (Chandy, Das, Wilson, & Rao, 2000).

The DS of ATRA controlled by the feed mole ratio of ATRA-NH_2 was calculated by measuring the content of ATRA in LHR conjugate using the UV method. The calculated DS of ATRA in LHR conjugate was shown in Table 1. The results indicated that the DS increased from 4.4% to 18.0% with the increase in the feed ratio of ATRA-NH_2.

CACs of LHR conjugate were determined by a fluorescence technique using pyrene as a probe. The CAC values of LHR conjugates decreased from 407 to 40 mg/L as the DS increased (Table 1), which was because higher hydrophobicity induced by more ATRA made a stronger hydrophobic interaction in the inner core of LHR conjugates.

Although some clinical trials suggested a beneficial effect of LMWH in cancer patients, LMWH-based therapy was difficult to manage due to its anticoagulant potency (Hirsh et al., 2001). The results in Table 1 showed that the anticoagulant activities of LHR conjugates decreased with the increase in DS. Especially for LHR-18 (the DS of ATRA was 18%), the anticoagulant activity was only about 30% versus native LMWH. It might be owing to the coupling of ATRA to the LMWH structure, as suggested in the study by Park et al. (2006), where the modified heparin with the carboxylic acid groups (e.g., uronic acid residues) had lower anticoagulant activity as compared to native heparin.

3.2. Preparation and characterization of LHR and PTX-loaded LHR nanoparticles

The LHR nanoparticles were prepared by a sonication method in aqueous condition. AFM and TEM studies showed that these nanoparticles were almost spherical in shape (Fig. 1(D)). DLS studies indicated that the particle size of LHR nanoparticles decreased from 430 to 140 nm with the increased DS (Table 1). The zeta

Table 1
Characterization of LHR conjugates.

Sample[a]	Feed mole ratio[b]	DS (%)	CAC (mg/L)	Size (nm)	Anticoagulant activity (%)[c]	
					FXa	aPTT
LHR-4	1:24:24	4.4	407	430	85.6	88.5
LHR-5	1:40:40	5.4	363	382	69.1	71.8
LHR-10	1:56:56	9.8	269	215	50.4	55.2
LHR-12	1:72:72	12.3	218	195	36.2	38.6
LHR-18	1:96:96	18.0	40	140	29.8	33.0

[a] LHR conjugates, where the number indicates the DS of ATRA.
[b] Mole ratio of LMWH:EDC:ATRA-NH_2.
[c] Anticoagulant activities of LHR conjugates were determined by established procedures for bioactivity assays with the FXa chromogenic assay and aPTT assay, respectively.

potentials were approximately −30 mV, indicating that negatively charged LMWH covered the nanoparticles.

The hydrophobic PTX was easily encapsulated into LHR nanoparticles by a dialysis method. The characteristics of PTX-loaded LHR nanoparticles with different DS of ATRA, including DL, EE and particle sizes, are summarized in Table 2. The DL enhanced with the increase of DS of ATRA in LHR. It should be emphasized that the maximum DL of PTX was as much as 33.1% with an EE of 93.1%, obtained from LHR-18 (the DS of ATRA was 18%, i.e., the content of ATAR was 10.0%). Such a high DL was considered as a result of the hydrophobic interactions between PTX and the hydrophobic region (ATRA) of the LHR nanoparticles.

The particle size of PTX-loaded LHR nanoparticles decreased with the increase of DS in the range of 228.0–108.9 nm, indicating that more compact hydrophobic cores had formed because of the increasing hydrophobic interaction. Moreover, the particle size of PTX-loaded LHR nanoparticles was smaller than its corresponding blank LHR nanoparticles, suggesting that the addition of hydrophobic drug could induce the nanoparticles more compact by the hydrophobic interaction between PTX and the hydrophobic segments of the nanoparticles.

DSC analysis of PTX-loaded LHR nanoparticles, PTX, physical mixture of PTX and LHR and LHR were carried out (figure not shown). PTX exhibited an endothermic melting peak at 224.2 °C and an exothermic decomposition peak at 244.5 °C, implying that PTX was in crystal status. The exothermic peak at 249.1 °C for LHR was attributed to the decomposed temperature of the modified conjugate. The characteristic DSC peaks of PTX and LHR do not exist in the thermograms of PTX-loaded LHR nanoparticles, but in those of physical mixture of PTX and LHR with small shifts at 216.6 °C and 241.1 °C. This suggested that PTX existed in the nanoparticles with the state of amorphism or solid dispersion.

3.3. *In vitro drug(s) release studies*

As reported in previous studies (Seow, Xue, & Yang, 2007), PTX and ATRA release were usually studied in PBS buffer solution in order to simulate *in vivo* biological environment. Thus, in this study, the *in vitro* release profiles of PTX-loaded LHR nanoparticles and PTX plus ATRA solution were obtained in pH 7.4 PBS at 37 °C and the results were shown in Fig. 2(A).

Table 2
Drug-loading (DL), entrapment efficiency (EE) and particle size of PTX-loaded LHR nanoparticles, data were represented as mean ± SD ($n = 5$).

Sample	DL (wt%)	EE (%)	Size (nm)
PTX-loaded LHR-4	1.4 ± 0.1	2.78 ± 0.2	228.0 ± 2.3
PTX-loaded LHR-5	3.9 ± 0.4	7.53 ± 0.5	154.4 ± 2.1
PTX-loaded LHR-10	31.6 ± 0.7	87.0 ± 1.1	123.0 ± 2.6
PTX-loaded LHR-12	32.0 ± 0.6	89.7 ± 2.1	119.6 ± 1.8
PTX-loaded LHR-18	33.1 ± 0.3	93.1 ± 1.9	108.9 ± 1.4

As can be seen, the drugs released fairly rapidly in PTX plus ATRA solution. Within 4 d, approximately 86% ATRA was released from the solution, and those for PTX approximately were 78%. But for the PTX-loaded LHR nanoparticles, both release profiles of PTX and ATRA exhibited a steady continued-release pattern and no initial burst release effect was observed. These results showed that the PTX-loaded LHR nanoparticles displayed the sustained release profiles. Furthermore, it can be concluded that the sustained release profiles are contributed to the nanoparticles formulation. Only about 13% of PTX was released over 10 d. It was also found that the rates of ATRA release were much slower than those of PTX at the same conditions and the release profiles were almost linear. For

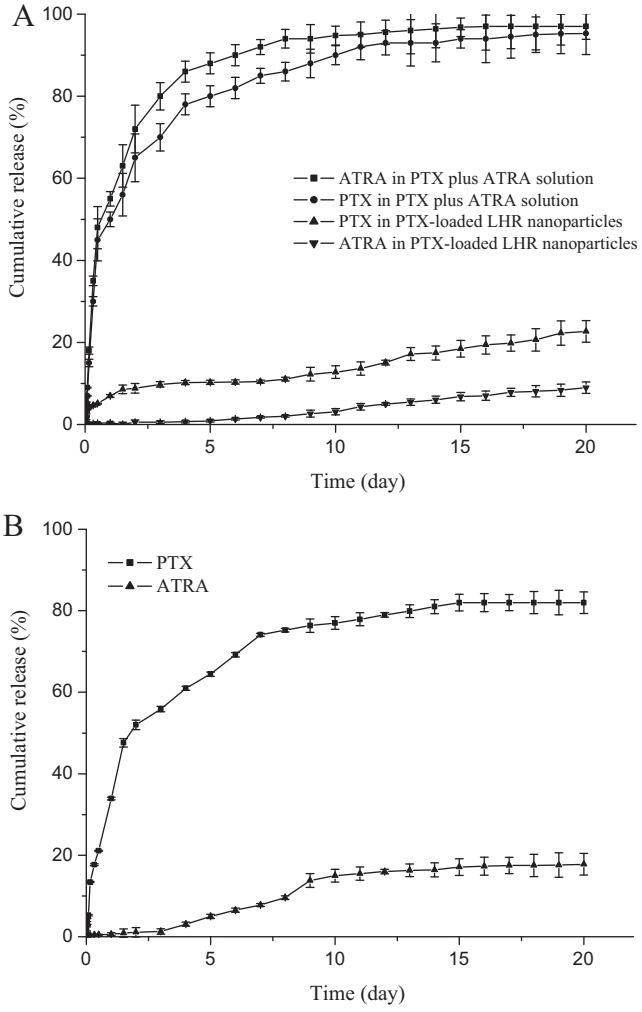

Fig. 2. (A) Release profiles of PTX and ATRA from PTX-loaded LHR nanoparticles and PTX plus ATRA solution at pH 7.4. (B) Release profiles of PTX and ATRA from PTX-loaded LHR nanoparticles at pH 5.8. Data are represented as mean ± SD, $n = 3$.

instance, within 4 d, only approximately 0.7% ATRA was released from nanoparticles, but those for PTX approximately was 10%. This was because ATRA was covalently combined to the matrix conjugate and its release was controlled by its dissociation from the conjugate chain rather than by simple diffusion.

Fig. 2(B) shows that the cumulative release of PTX and ATRA increased in the acidic media, especially for PTX. About 56% of PTX has been released within 48 h. The results indicated that the drugs could be released from the PTX-loaded LHR nanoparticles at the mildly acidic pH in tumor as well as in the endosomal and lysosomal compartments of cells (Rijcken, Soga, Hennink, & van Nostrum, 2007).

3.4. Hydrolysis study of LHR nanoparticles and stability of PTX-loaded LHR nanoparticles in plasma

The ideal drug delivery system stably retains the entrapped drug in the bloodstream, and releases the drug only after reaching the site of action (Rijcken, Soga, Hennink, & van Nostrum, 2007). In this study, the hydrolysis of LHR conjugates and the stability of PTX-loaded LHR nanoparticles in plasma were investigated. The result showed that LHR undergone very slow enzymatic release in plasma, which was reflected in the release of only about 3.1% of ATRA in 48 h. Furthermore, about 90% of PTX was detected in plasma at 48 h after incubating, which demonstrated that PTX in the nanoparticles maintained stable.

3.5. In vitro cytotoxicity studies

The effect of LHR nanoparticles on PTX-induced cytotoxicity was investigated in HepG2 cell line by the MTT assay. It was shown that LHR at the studied concentration range slightly decreased cell viability, suggesting that LHR was not cytotoxic against HepG2 cells. Therefore, the possibility that LHR nanoparticles were responsible for the cytotoxicity was eliminated. When LHR and PTX were concurrently treated in the form of PTX-loaded LHR nanoparticles, the IC_{50} against HepG2 was 0.119 μg/mL, whereas the IC_{50} of PTX solution was 0.307 μg/mL. This result indicated that PTX-loaded LHR nanoparticles exhibited higher cytotoxic activity *in vitro* than PTX solution. In addition, a dose-dependent change in cytotoxicity was observed in Fig. 3(a).

In order to confirm whether the enhanced cytotoxicity of nanoparticles was due to ATRA-mediated PTX sensitization (Pratt, Niu, & Renart, 2006), we similarly determined the effect of PTX plus ATRA solution on HepG2. It was found that PTX plus ATRA solution (IC_{50} ~0.159 μg/mL) was more effective than PTX solution, implying a synergistic or additive effect of PTX and ATRA in the HepG2 cell, which was consistent with the research carried out by Wang, Yang, Uytingco, Christakos, and Wieder (2000). Moreover, PTX-loaded LHR nanoparticles displayed slightly higher *in vitro* cytotoxicity as compared to PTX plus ATRA solution.

The results were even better if the sustainable drug-release feature of the nanoparticles was taken into account. The mortality of the cells treated by the nanoparticles should be corrected by the accumulated drug release (Dong & Feng, 2007).

$$\text{Modified mortality} = \frac{\text{Measured mortality}}{\text{Accumulated drug release}} \times 2$$

Fig. 2 shows that 9.8% of PTX and 0.5% of ATRA loaded in the PTX-loaded LHR nanoparticles was released out after 72 h. As a result, after corrected by the drug release, the modified mortality of PTX-loaded LHR nanoparticles were 21.1 times than that those of the PTX plus ATRA solution at equivalent PTX and ATRA concentration of 1 μg/mL and 0.2 μg/mL after 72 h treatment. However, it seemed that the cytotoxicity of the PTX-loaded LHR nanoparticles versus PTX plus ATRA solution was less significant at high drug concentration. The reason could be due to the adjuvant cremophor EL and ethanol in the PTX plus ATRA solution, since it was found an obviously reduction in cells viability when the cells were incubated with pure cremophor EL at high concentration (Fonseca, Simoes, & Gaspar, 2002).

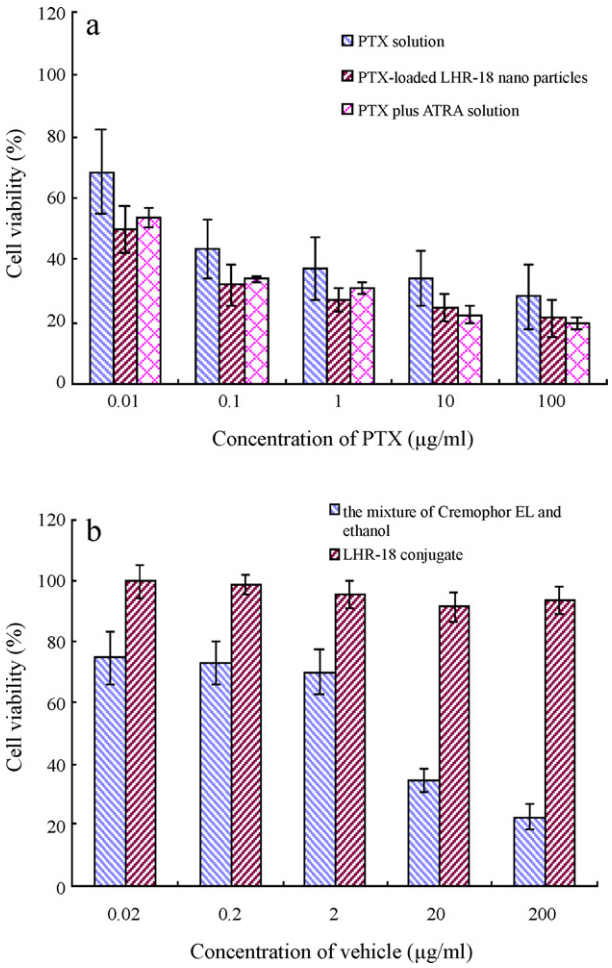

Fig. 3. Viability of HepG2 cells as a function of PTX concentration of PTX solution, PTX-loaded LHR-18 nanoparticles and PTX plus ATRA solution (a), and corresponding concentration of the vehicle of PTX plus ATRA solution and LHR-18 conjugate (b). Data represent mean ± SD, $n = 6$.

3.6. Hemolysis test

The hemolysis of LHR conjugate was compared with the mixture of cremophor EL and ethanol, and Tween-80. As shown in Fig. 4(a), the hemolysis of LHR conjugate was negligible, which was similar to the mixture of cremophor EL and ethanol. As the concentration increased, hemolysis induced by Tween-80 increased dramatically, and reached 31.8% at the concentration of 0.6 mg/mL. However, cremophor EL is considered more dangerous than Tween-80, which might account for the serious effects, such as hypersensitivity and neurotoxicity (Huo, Zhang, Zhou, Zou, & Li, 2010). Meanwhile, the hemolysis of PTX-loaded LHR nanoparticles was compared with the PTX plus ATRA solution (Fig. 4(b)). PTX-loaded LHR nanoparticles demonstrated an insignificant hemolytic activity, with only 1.4% at the concentration of 0.2 mg PTX/mL and 0.04 mg ATRA/mL. But the hemolysis by PTX plus ATRA solution was 11.2% at the same concentration. These results suggested that LHR conjugate and PTX-loaded LHR nanoparticles would be non-toxic towards erythrocytes after intravenous injection.

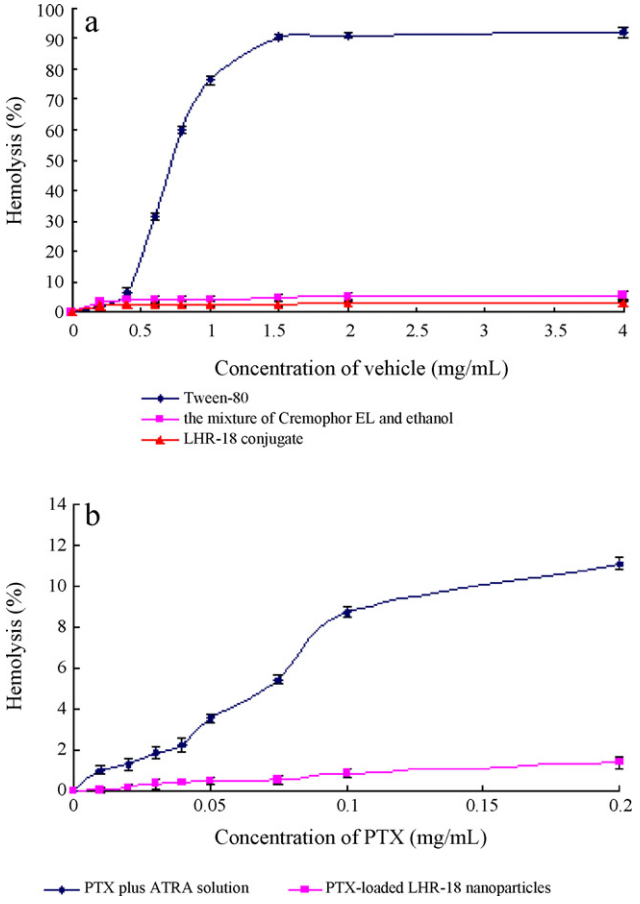

Fig. 4. Hemolysis as a function of vehicle concentration of LHR-18, the mixture of cremophor EL and ethanol, and Tween-80 (a), and PTX concentration of PTX-loaded LHR-18 nanoparticles and PTX plus ATRA solution (b). Data represent mean ± SD, $n = 3$.

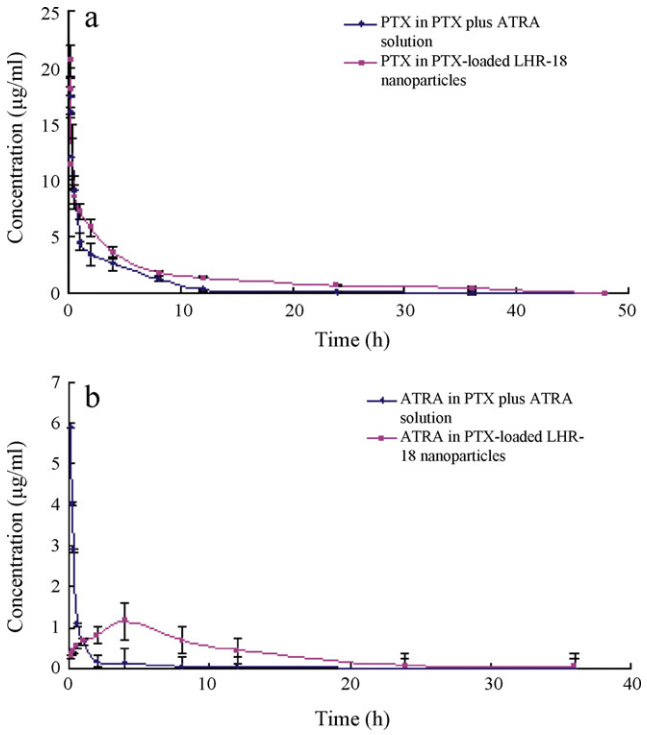

Fig. 5. Plasma concentration–time curves of PTX (a) and ATRA (b) encapsulated in PTX plus ATRA solution and PTX-loaded LHR-18 nanoparticles following the i.v. administration of a single dose of 8 mg PTX/kg and 1.6 mg ATRA/kg in Sprague–Dawley rats. The data represent the mean ± SD, $n = 5$.

3.7. Pharmacokinetic study

The plasma concentration–time profiles of PTX and ATRA after i.v. administration of PTX-loaded LHR-18 nanoparticles and PTX plus ATRA solution were shown in Fig. 5. After i.v. administration, PTX from the PTX plus ATRA solution was quickly remove from the circulating system. On the contrary, PTX-loaded LHR-18 nanoparticles exhibited a delayed blood clearance. It could be seen that the PTX level from the nanoparticles remained higher at all time points compared with those of PTX from PTX plus ATRA solution. In addition, PTX and ATRA were detectable in the plasma up to 24 h for PTX-loaded LHR-18 nanoparticles, whereas they were undetectable beyond 12 h and 8 h, respectively, for PTX plus ATRA solution, implying stability in the bloodstream and maintenance of an intact nanostructure (Cho et al., 2007).

According to the actual data from the experiment, AUC_{0-24} was calculated by logarithmic trapezoidal methods. It was shown that AUC_{0-24} and MRT of PTX in nanoparticles were found to be higher than those in the solution formulation ($p < 0.05$) (1.86- and 1.92-fold increase).

The pharmacokinetic parameters, obtained by statistical moment analysis, were summarized in Table 3. PTX-loaded LHR-18 nanoparticles significantly changed the pharmacokinetic parameters of the drugs in comparison with PTX plus ATRA solution ($p < 0.05$), as expected. The total area-under-the-curve (AUC), which determined the therapeutic effects, and mean residence time (MRT) of PTX and ATRA in PTX-loaded LHR-18 nanoparticles were found to be higher than those in the PTX plus ATRA solution ($p < 0.05$) (2.0- and 2.38-fold increase for PTX, and 3.75- and 4.68-fold increase for ATRA, respectively). On the other hand, the clearance of PTX and ATRA in PTX-loaded LHR nanoparticles decreased 1.79- and 3.65-fold, respectively, compared to that in PTX plus ATRA solution. The results indicated that PTX-loaded LHR nanoparticles were attributed to an extended circulation of PTX and ATRA, and might contribute to the improved therapeutic efficacy.

4. Discussion

Clinical protocols for cancer chemotherapy rarely use a single drug but usually combine two or more drugs with different mechanisms of action (Ajani, 2006). For simultaneously delivery of these anticancer drugs, polymer–drug conjugate is considered as one of the most promising DDS for combination chemotherapy. In addition to improve the poor solubility associated with many cancer chemotherapeutic drugs, it can also prolong the circulation time, achieve controlled or sustained drug release, and accumulate in

Table 3
Pharmacokinetic parameters of PTX and ATRA after i.v. injection of the PTX plus ATRA solution and PTX-loaded LHR-18 nanoparticles in Sprague–Dawley rats at a dose of 8 mg PTX/kg and 1.6 mg ATRA/kg ($n = 5$).

	AUC (μg h/mL)[a]	CL (mL/h)[b]	MRT (h)[c]
PTX plus ATRA solution			
PTX	36.82 ± 3.13	43.45 ± 4.14	4.97 ± 0.96
ATRA	3.49 ± 0.12	91.79 ± 3.24	2.88 ± 0.25
PTX-loaded LHR-18 nanoparticles			
PTX	73.87 ± 4.21*	24.23 ± 2.11*	11.84 ± 1.23**
ATRA	13.09 ± 1.56**	25.15 ± 2.33**	13.49 ± 0.92**

[a] Area under the curve.
[b] Clearance.
[c] Mean residence time.
* $P < 0.05$ vs. PTX plus ATRA solution.
** $P < 0.01$ vs. PTX plus ATRA solution.

the tumor sites and thereby maximize the therapeutic index and minimize non-specific toxicity.

In this study, LHR conjugate, comprised of covalently bound LMWH as a hydrophilic segment and ATRA as a hydrophobic segment, was prepared for delivering two different anticancer drugs simultaneously. The modification of carboxylic groups in LMWH resulted in a significant decrease in its anticoagulant activity, and could decrease side effects such as heparin-induced thrombocytopenia (HIT) or bleeding (Dager & White, 2004). Furthermore, through the intact sulfate group, the conjugated LMWH retained its ability to inhibit binding with angiogenic factors, which could induce proliferation of smooth muscle cells (Cho et al., 2008). Encouragingly, LHR conjugate has illustrated a high tendency for self-assembly reflected by a relatively low CAC (Table 1). They could form self-assembled nanoparticles bearing a hydrophobic inner core that could be served as a container for hydrophobic drugs. Herein, PTX can be easily entrapped into LHR nanoparticles, as summarized in Table 2. The DL of PTX in LHR-18 nanoparticles was high up to about 33.1% with a high drug EE, which was greater than some other reported nanoparticles, such as pHPMAmDL-*b*-PEG (Soga et al., 2005). By conjugating ATRA to LMWH and incorporating PTX into LHR nanoparticles, the solubility and simultaneous delivery problems could be both overcome.

It has been reported that ATRA at low doses could be as effective as conventional doses used in various tumors (Castaigne et al., 1993; Chen et al., 1996). Furthermore, the commonly clinical dose of PTX and ATRA is 135–175 mg/m^2 and 20–40 mg/m^2, respectively. In other word, the drug ratio of PTX and ATRA is about 8:1 to 4:1. In our study, PTX-loaded LHR-18 nanoparticles are just consistent with the commonly clinical dose. Therefore, the LHR-18 was selected for the later studies. Moreover, the anticoagulant activity assay showed that the anticoagulant activity of LHR-18 was only about 30% versus native LMWH. Thus, LHR-18 with such low anticoagulant activities could be a safer and more effective drug delivery system which could markedly decrease the high risk of excessive bleeding at the current dose regimen. Nevertheless, side effects should be also taken into consideration at high dosages because of its residuary anticoagulant activity.

Since free PTX is more rapidly cleared *in vivo* (Wu, Liu, & Lee, 2006), this factor might have a negative effect on the therapeutic efficacy. In our studies, pharmacokinetic studies on the PTX and ATRA of PTX-loaded LHR nanoparticles indicated a longer systemic circulation time relative to that of PTX plus ATRA solution, as suggested in the study of glycol chitosan nanoparticles by Park, Kim, Nan, et al. (2007), where glycol chitosan nanoparticles displayed prolonged blood circulation time and decreased time-dependent excretion from the body. It was considered that the characteristic properties of the nanoparticles played a key role here. Firstly, low CAC values of LHR can make the formation of nanoparticles easier even under highly diluted conditions, and these nanoparticles can preserve stability without dissociation after intravenous injected into the larger volume of blood for systemic circulation (Zhang, Huo, Zhou, Yu, & Wu, 2009). Secondly, the particle size of PTX-loaded LHR nanoparticles (the DS of 18% was taken as example) was about 108.9 nm with narrow size distribution. It was reported that the particles with the size of around 100–150 nm were preferred to avoid easily the non-selective recognition by the reticuloendothelial system (RES) (Takeuchi, Kojima, Yamamoto, & Kawashima, 2000) and achieve tumor targeting by EPR effect (Kohane, 2007). Finally, as some researches reported (Han et al., 2006), heparin which was fixed on the nanoparticles surface could shelter drug from the serum proteins and prolonged its half-life.

Moreover, the results of PTX and ATRA release kinetics as well as their stability assay in plasma showed that the nanoparticles could prevent the premature release of drugs, exhibit sustained release profiles in physiological conditions (pH 7.4, 37 °C) (Fig. 2) and maintain drugs stable in the plasma. The results were perhaps due to high hydrophobicity of the nanoparticle core (Saravanakumar et al., 2009), which retarded the diffusion of water into the core, and prevented subsequent diffusion of PTX localized in the core and cleavage of the hydrolysable ester bonds between LMWH and ATRA. Consequently, PTX-loaded LHR nanoparticles were expected to retain drugs while circulating, thereby preventing premature drug release before the nanoparticles accumulated in the tumor (Min et al., 2008).

Several investigations have demonstrated that the combination of ATRA with PTX most effectively down-regulated survival factors and activated mitochondria-dependent multiple pathways for apoptosis (Karmakar, Banik, & Ray, 2008). In this study, the cytotoxicity results showed that the combination of PTX with ATRA in the form of PTX-loaded LHR nanoparticles significantly enhanced the cytotoxicity ($P < 0.01$) compared to the PTX solution, as suggested in the research by Muindi (1996), where PTX-induced cytotoxicity could be enhanced by ATRA. Furthermore, a slightly enhanced cytotoxicity compared to PTX plus ATRA solution was observed in the study. Free drugs are supposed to be transported into cells by passive diffusion, but nanoparticles are likely to be internalized within cells via endocytosis (Park, Kim, Tran, Huh, & Lee, 2010). The higher toxicity of PTX-loaded LHR nanoparticles might be attributed to its greater uptake and accumulation in cancer cells compared to free PTX and ATRA. In addition, the enhancement of PTX activity mediated by its incorporation into nanoparticles may be explained by the fact that these systems can act as a reservoir for PTX and ATRA, protecting the drug from epimerization and hydrolysis (Dordunoo & Burt, 1996) and providing not only a sustained release of PTX and ATRA, but also contributing to the maintenance of their activity (Fonseca, Simoes, & Gaspar, 2002).

The potential toxicity is an important consideration in nanoparticle development (Wang, Li, et al., 2009). Since LHR conjugate was aimed to be used as an intravenous injectable nanocarrier for PTX, the toxicity was evaluated by hemolysis test and *in vitro* cytotoxicity studies. As the hemolysis results suggested, LHR conjugate and PTX-loaded LHR nanoparticles showed no significant effects on hemolysis. In addition, given the toxicity associated with common formulation vehicles used, like cremophor EL and ethanol, PTX-loaded LHR nanoparticles provided a safer and less toxic alternative. The *in vitro* cytotoxicity study demonstrated that no cytotoxicity of LHR conjugate (up to 200 μg/mL) was observed in HepG2 cells. In contrast, the vehicle for PTX plus ATRA solution, cremophor EL and ethanol, had severe cytotoxicity at the relevant concentration.

Moreover, LHR conjugate with a high negative charge and hydrophobic segment may strongly interact with various proteins, more efficiently blocking the biological activities of proteins compared to other heparin derivatives (Park, Kim, Lee, et al., 2007). Therefore, PTX-loaded LHR nanoparticles are more applicable and have high potential for combination cancer chemotherapy.

5. Conclusions

Amphiphilic LHR conjugate was successfully developed, which could self-assemble to form stable nanoparticles and readily encapsulate hydrophobic drugs such as PTX with a high DL and EE. It was shown that we could combine up two chemotherapeutic agents (PTX and ATRA) in one carrier system. PTX-loaded LHR nanoparticles presented a sustained drug release profile and significantly enhanced *in vitro* antitumor activity. The hemolysis and cytotoxicity studies, which showed that LHR conjugate was safer than the mixture of cremophor EL and ethanol, added evidence to use the LHR conjugate as an intravenous injectable material. In animal studies, PTX-loaded LHR nanoparticles possessed prolonged circulation time compared to PTX plus ATRA solution. This investigation

suggested an important potential clinical application of the combination regimen in cancer treatment. It could be concluded that LHR conjugate is a promising candidate as a drug carrier for combination cancer chemotherapy of PTX and ATRA.

Acknowledgements

This work was supported by the Major Project of National Science and Technology of China for New Drugs Development (No. 2009ZX09310-004), the National Basic Research Program of China (No. 2009CB930303), and by the Fundamental Research Funds for the Central Universities (Program No. JKY2009018). This work was carried out at State Key Laboratory of Natural Medicines (China Pharmaceutical University).

References

Ajani, J. A. (2006). Chemotherapy for advanced gastric or gastroesophageal cancer: Defining the contributions of docetaxel. *Expert Opinion on Pharmacotherapy*, *7*(12), 1627–1631.

Arrieta, O., Gonzalez-De la Rosa, C. H., Arechaga-Ocampo, E., Villanueva-Rodriguez, G., Ceron-Lizarraga, T. L., Martinez-Barrera, L., et al. (2010). Randomized phase II trial of all-*trans*-retinoic acid with chemotherapy based on paclitaxel and cisplatin as first-line treatment in patients with advanced non-small-cell lung cancer. *Journal of Clinical Oncology*, *28*(21), 3463–3471.

Bae, Y., Diezi, T. A., Zhao, A., & Kwon, G. S. (2007). Mixed polymeric micelles for combination cancer chemotherapy through the concurrent delivery of multiple chemotherapeutic agents. *Journal of Controlled Release*, *122*(3), 324–330.

Castaigne, S., Lefebvre, P., Chomienne, C., Suc, E., Rigal-Huguet, F., Gardin, C., et al. (1993). Effectiveness and pharmacokinetics of low-dose all-*trans* retinoic acid (25 mg/m^2) in acute promyelocytic leukemia. *Blood*, *82*(12), 3560–3563.

Ceruti, M., Crosasso, P., Brusa, P., Arpicco, S., Dosio, F., & Cattel, L. (2000). Preparation, characterization, cytotoxicity and pharmacokinetics of liposomes containing water-soluble prodrugs of paclitaxel. *Journal of Controlled Release*, *63*(1–2), 141–153.

Chandy, T., Das, G. S., Wilson, R. F., & Rao, G. H. (2000). Use of plasma glow for surface-engineering biomolecules to enhance bloodcompatibility of Dacron and PTFE vascular prosthesis. *Biomaterials*, *21*(7), 699–712.

Chen, G. Q., Shen, Z. X., Wu, F., Han, J. Y., Miao, J. M., Zhong, H. J., et al. (1996). Pharmacokinetics and efficacy of low-dose all-*trans* retinoic acid in the treatment of acute promyelocytic leukemia. *Leukemia*, *10*(5), 825–828.

Cho, K. J., Moon, H. T., Park, G. E., Jeon, O. C., Byun, Y., & Lee, Y. K. (2008). Preparation of sodium deoxycholate (DOC) conjugated heparin derivatives for inhibition of angiogenesis and cancer cell growth. *Bioconjugate Chemistry*, *19*(7), 1346–1351.

Cho, Y. W., Park, S. A., Han, T. H., Son, D. H., Park, J. S., Oh, S. J., et al. (2007). *In vivo* tumor targeting and radionuclide imaging with self-assembled nanoparticles: Mechanisms, key factors, and their implications. *Biomaterials*, *28*(6), 1236–1247.

Dager, W. E., & White, R. H. (2004). Low-molecular-weight heparin-induced thrombocytopenia in a child. *Annals of Pharmacotherapy*, *38*(2), 247–250.

Dong, Y., & Feng, S. S. (2007). *In vitro* and *in vivo* evaluation of methoxy polyethylene glycol–polylactide (MPEG–PLA) nanoparticles for small-molecule drug chemotherapy. *Biomaterials*, *28*(28), 4154–4160.

Dordunoo, S. K., & Burt, H. M. (1996). Solubility and stability of taxol: Effects of buffers and cyclodextrins. *International Journal of Pharmaceutics*, *133*, 191–201.

Fonseca, C., Simoes, S., & Gaspar, R. (2002). Paclitaxel-loaded PLGA nanoparticles: Preparation, physicochemical characterization and *in vitro* anti-tumoral activity. *Journal of Controlled Release*, *83*(2), 273–286.

Garnett, M. C. (2001). Targeted drug conjugates: Principles and progress. *Advanced Drug Delivery Reviews*, *53*(2), 171–216.

Go, D. H., Joung, Y. K., Park, S. Y., Park, Y. D., & Park, K. D. (2008). Heparin-conjugated star-shaped PLA for improved biocompatibility. *Journal of Biomedical Materials Research A*, *86*(3), 842–848.

Godwin, A., Bolina, K., Clochard, M., Dinand, E., Rankin, S., Simic, S., et al. (2001). New strategies for polymer development in pharmaceutical science—A short review. *Journal of Pharmacy and Pharmacology*, *53*(9), 1175–1184.

Greco, F., & Vicent, M. J. (2009). Combination therapy: Opportunities and challenges for polymer–drug conjugates as anticancer nanomedicines. *Advanced Drug Delivery Reviews*, *61*(13), 1203–1213.

Han, H. D., Lee, A., Song, C. K., Hwang, T., Seong, H., Lee, C. O., et al. (2006). *In vivo* distribution and antitumor activity of heparin-stabilized doxorubicin-loaded liposomes. *International Journal of Pharmaceutics*, *313*(1–2), 181–188.

Hawkins, M. J., Soon-Shiong, P., & Desai, N. (2008). Protein nanoparticles as drug carriers in clinical medicine. *Advanced Drug Delivery Reviews*, *60*(8), 876–885.

Hirsh, J., Warkentin, T. E., Shaughnessy, S. G., Anand, S. S., Halperin, J. L., Raschke, R., et al. (2001). Heparin and low-molecular-weight heparin: Mechanisms of action, pharmacokinetics, dosing, monitoring, efficacy, and safety. *Chest*, *119*(1 Suppl.), 64S–94S.

Huo, M., Zhang, Y., Zhou, J., Zou, A., & Li, J. (2010). Formation, microstructure, biodistribution and absence of toxicity of polymeric micelles formed by N-octyl-N,O-carboxymethyl chitosan. *Carbohydrate Polymers*, *83*(4), 1959–1969.

Jee, K. S, Park, H. D., Park, K. D., Kim, Y. H., & Shin, J. W. (2004). Heparin conjugated polylactide as a blood compatible material. *Biomacromolecules*, *5*(5), 1877–1881.

Kan, P., Chen, Z. B., Lee, C. J., & Chu, I. M. (1999). Development of nonionic surfactant/phospholipid o/w emulsion as a paclitaxel delivery system. *Journal of Controlled Release*, *58*(3), 271–278.

Karmakar, S., Banik, N. L., & Ray, S. K. (2008). Combination of all-*trans* retinoic acid and paclitaxel-induced differentiation and apoptosis in human glioblastoma U87MG xenografts in nude mice. *Cancer*, *112*(3), 596–607.

Kohane, D. S. (2007). Microparticles and nanoparticles for drug delivery. *Biotechnology and Bioengineering*, *96*(2), 203–209.

Le Garrec, D., Gori, S., Luo, L., Lessard, D., Smith, D. C., Yessine, M. A., et al. (2004). Poly(N-vinylpyrrolidone)-block-poly(D,L-lactide) as a new polymeric solubilizer for hydrophobic anticancer drugs: *In vitro* and *in vivo* evaluation. *Journal of Controlled Release*, *99*(1), 83–101.

Lee, Y., Moon, H. T., & Byun, Y. (1998). Preparation of slightly hydrophobic heparin derivatives which can be used for solvent casting in polymeric formulation. *Thrombosis Research*, *92*(4), 149–156.

Lee, Y., Nam, J. H., Shin, H. C., & Byun, Y. (2001). Conjugation of low-molecular-weight heparin and deoxycholic acid for the development of a new oral anticoagulant agent. *Circulation*, *104*(25), 3116–3120.

Min, K. H., Park, K., Kim, Y. S., Bae, S. M., Lee, S., Jo, H. G., et al. (2008). Hydrophobically modified glycol chitosan nanoparticles-encapsulated camptothecin enhance the drug stability and tumor targeting in cancer therapy. *Journal of Controlled Release*, *127*(3), 208–218.

Muindi, J. R. (1996). Retinoids in clinical cancer therapy. *Cancer Treatment and Research*, *87*, 305–342.

Park, I.-K., Kim, Y. J., Tran, T. H., Huh, K. M., & Lee, Y. k. (2010). Water-soluble heparin-PTX conjugates for cancer targeting. *Polymer*, *51*, 3387–3393.

Park, K., Kim, J. H., Nam, Y. S., Lee, S., Nam, H. Y., Kim, K., et al. (2007). Effect of polymer molecular weight on the tumor targeting characteristics of self-assembled glycol chitosan nanoparticles. *Journal of Controlled Release*, *122*(3), 305–314.

Park, K., Kim, Y. S., Lee, G. Y., Nam, J. O., Lee, S. K., Park, R. W., et al. (2007). Antiangiogenic effect of bile acid acylated heparin derivative. *Pharmaceutical Research*, *24*(1), 176–185.

Park, K., Kim, Y. S., Lee, G. Y., Park, R. W., Kim, I. S., Kim, S. Y., et al. (2008). Tumor endothelial cell targeted cyclic RGD-modified heparin derivative: Inhibition of angiogenesis and tumor growth. *Pharmaceutical Research*, *25*(12), 2786–2798.

Park, K., Lee, G. Y., Kim, Y. S., Yu, M., Park, R. W., Kim, I. S., et al. (2006). Heparin-deoxycholic acid chemical conjugate as an anticancer drug carrier and its antitumor activity. *Journal of Controlled Release*, *114*(3), 300–306.

Park, K., Lee, G. Y., Park, R. W., Kim, I. S., Kim, S. Y., & Byun, Y. (2008). Combination therapy of heparin-deoxycholic acid conjugate and doxorubicin against squamous cell carcinoma and B16F10 melanoma. *Pharmaceutical Research*, *25*(2), 268–276.

Pratt, M. A., Niu, M. Y., & Renart, L. I. (2006). Regulation of survivin by retinoic acid and its role in paclitaxel-mediated cytotoxicity in MCF-7 breast cancer cells. *Apoptosis*, *11*(4), 589–605.

Rihova, B. (2002). Immunomodulating activities of soluble synthetic polymer-bound drugs. *Advanced Drug Delivery Reviews*, *54*(5), 653–674.

Rijcken, C. J., Soga, O., Hennink, W. E., & van Nostrum, C. F. (2007). Triggered destabilisation of polymeric micelles and vesicles by changing polymers polarity: An attractive tool for drug delivery. *Journal of Controlled Release*, *120*(3), 131–148.

Rowinsky, E. K., & Donehover, R. C. (1995). Paclitaxel (Taxol). *New England Journal of Medicine*, *332*, 1004–1014.

Sadikoglou, E., Magoulas, G., Theodoropoulou, C., Athanassopoulos, C. M., Giannopoulou, E., Theodorakopoulou, O., et al. (2009). Effect of conjugates of all-*trans*-retinoic acid and shorter polyene chain analogues with amino acids on prostate cancer cell growth. *European Journal of Medical Chemistry*, *44*(8), 3175–3187.

Safavy, A., Bonner, J. A., Waksal, H. W., Buchsbaum, D. J., Gillespie, G. Y., Khazaeli, M. B., et al. (2003). Synthesis and biological evaluation of paclitaxel-C225 conjugate as a model for targeted drug delivery. *Bioconjugate Chemistry*, *14*(2), 302–310.

Saravanakumar, G., Min, K. H., Min, D. S., Kim, A. Y., Lee, C. M., Cho, Y. W., et al. (2009). Hydrotropic oligomer-conjugated glycol chitosan as a carrier of paclitaxel: Synthesis, characterization, and *in vivo* biodistribution. *Journal of Controlled Release*, *140*(3), 210–217.

Sato, H., Wang, Y. M., Adachi, I., & Horikoshi, I. (1996). Pharmacokinetic study of taxol-loaded poly(lactic-co-glycolic acid) microspheres containing isopropyl myristate after targeted delivery to the lung in mice. *Biological and Pharmaceutical Bulletin*, *19*(12), 1596–1601.

Segal, E., & Satchi-Fainaro, R. (2009). Design and development of polymer conjugates as anti-angiogenic agents. *Advanced Drug Delivery Reviews*, *61*(13), 1159–1176.

Seow, W. Y., Xue, J. M., & Yang, Y. Y. (2007). Targeted and intracellular delivery of paclitaxel using multi-functional polymeric micelles. *Biomaterials*, *28*(9), 1730–1740.

Soga, O., van Nostrum, C. F., Fens, M., Rijcken, C. J., Schiffelers, R. M., Storm, G., et al. (2005). Thermosensitive and biodegradable polymeric micelles for paclitaxel delivery. *Journal of Controlled Release*, *103*(2), 341–353.

Sun, J., Huang, H., Zhu, Y., Lan, J., Li, J., Lai, X., et al. (2005). The expression of telomeric proteins and their probable regulation of telomerase during the differentiation of all-*trans*-retinoic acid-responsive and -resistant acute promyelocytic leukemia cells. *International Journal of Hematology*, *82*(3), 215–223.

Takeuchi, H., Kojima, H., Yamamoto, H., & Kawashima, Y. (2000). Polymer coating of liposomes with a modified polyvinyl alcohol and their systemic circulation and RES uptake in rats. *Journal of Controlled Release*, *68*(2), 195–205.

Tiersten, A. D., Selleck, M. J., Hershman, D. L., Smith, D., Resnik, E. E., Troxel, A. B., et al. (2004). Phase II study of topotecan and paclitaxel for recurrent, persistent, or metastatic cervical carcinoma. *Gynecologic Oncology*, *92*(2), 635–638.

Ueda, Y., Yamagishi, H., Ichikawa, D., Okamoto, K., Otsuji, E., Morii, J., et al. (2010). Multicenter phase II study of weekly paclitaxel plus S-1 combination chemotherapy in patients with advanced gastric cancer. *Gastric Cancer*, *13*(3), 149–154.

Wang, Q., Yang, W., Uytingco, M. S., Christakos, S., & Wieder, R. (2000). 1,25-Dihydroxyvitamin D3 and all-*trans*-retinoic acid sensitize breast cancer cells to chemotherapy-induced cell death. *Cancer Research*, *60*(7), 2040–2048.

Wang, X., Li, J., Wang, Y., Cho, K. J., Kim, G., Gjyrezi, A., et al. (2009). HFT-T, a targeting nanoparticle, enhances specific delivery of paclitaxel to folate receptor-positive tumors. *ACS Nano*, *3*(10), 3165–3174.

Wang, Y., Xin, D., Liu, K., Zhu, M., & Xiang, J. (2009). Heparin-paclitaxel conjugates as drug delivery system: Synthesis, self-assembly property, drug release, and antitumor activity. *Bioconjugate Chemistry*, *20*(12), 2214–2221.

Wu, J., Liu, Q., & Lee, R. J. (2006). A folate receptor-targeted liposomal formulation for paclitaxel. *International Journal of Pharmaceutics*, *316*(1–2), 148–153.

Zacharski, L. R., & Ornstein, D. L. (1998). Heparin and cancer. *Thrombosis and Haemostasis*, *80*(1), 10–23.

Zeng, J., Yang, L., Liang, Q., Zhang, X., Guan, H., Xu, X., et al. (2005). Influence of the drug compatibility with polymer solution on the release kinetics of electrospun fiber formulation. *Journal of Controlled Release*, *105*(1–2), 43–51.

Zhang, Y., Huo, M., Zhou, J., Yu, D., & Wu, Y. (2009). Potential of amphiphilically modified low molecular weight chitosan as a novel carrier for hydrophobic anticancer drug: Synthesis, characterization, Micellization and cytotoxicity evaluation. *Carbohydrate Polymers*, *77*(2), 231–238.